Response of a Swirled Non-Premixed Burner to Fuel Flow Rate Modulation

A. X. Sengissen[1], T. J. Poinsot[2], J. F. Van Kampen[3], and J. B. W. Kok[3]

[1] CERFACS, 42 Av. G. Coriolis, 31057 Toulouse cedex, France
Alois.Sengissen@cerfacs.fr
[2] IMFT, Allée du Professeur C. Soula, 31400 Toulouse, France
Thierry.Poinsot@imft.fr
[3] University of Twente, 7500 AE Enschede, The Netherlands
J.B.W.Kok@ctw.utwente.nl

Summary. Combustion instability studies require the identification of the combustion chamber response. In non-premixed devices, the combustion processes are influenced by oscillations of the air flow rate but may also be sensitive to fluctuations of the fuel flow rate entering the chamber. This paper describes a numerical study of the mechanisms controlling the response of a swirled non-premixed combustor burning natural gas and air. The flow is first characterized without combustion and LDV results are compared to Large Eddy Simulation (LES) data. The non-pulsated reacting regime is then studied and characterized in terms of fields of heat release and equivalence ratio. Finally the combustor fuel flow rate is pulsated at several amplitudes and the response of the chamber is analyzed using phase-locked averaging and first order acoustic analysis.

1 Introduction

Many combustors exhibit combustion instabilities which constitute significant risks for project developments. Being able to predict the stability of a given burner is the center of many present research programs: these efforts can be experimental [1–10] or numerical [11–14]. A specificity of modern gas turbines is that these systems operate in very lean regimes to satisfy emission regulations. The resulting flames are extremely sensitive to combustion oscillations but the exact phenomena leading to instabilities are still a matter of discussions. A central question for modeling approaches is to know what induces an unsteady reaction rate (necessary to sustain the oscillations) when an acoustic wave enters the combustion chamber. This mechanism described in figure 1 may be due to (at least) two main effects:

1. The formation of vortices in the combustion chamber (Fig. 1-a): These vortices are usually triggered by strong acoustic waves propagating in the

air passages. These structures capture large pockets of fresh gases which burn only later in a violent process leading to small scale turbulence and high reaction rates [15, 16].

2. The modification of the fuel and oxidizer flow rates when the acoustic wave propagates into the fuel and air feeding lines (Fig. 1-b). This can lead to a local change of the equivalence ratio (rich and poor pockets) and therefore to a modification of the burning rate when these pockets enter the chamber. If the burner operates in a very lean mode, this effect may be important since variations of inlet ratio may trigger strong combustion oscillations [17].

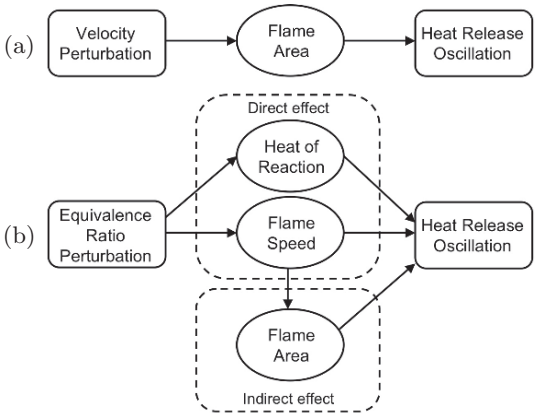

Fig. 1. Mechanism of the flame response to (a) velocity perturbations and (b) equivalence ratio perturbations.

In premixed combustors, the second mechanism has been identified as a key element controlling combustor stability [6, 17] but its effect on non-premixed devices remains unclear. According to Lieuwen, the mechanism is the following: even away from Lean or Rich Blow Off (LBO or RBO), equivalence ratio fluctuations produce very large heat-release oscillations which trigger combustion instabilities through pressure oscillations feedback. A direct proof of the importance of fuel injection on stability is that the location of fuel injectors often alters the stability of the system. The crucial role of fuel modulation can also be readily identified by considering active control examples in which a small modulation of the fuel lines feeding a combustor can be sufficient to alter the stability of the combustor [18–20].

Even though the general idea of the mechanism proposed by Lieuwen is fairly clear, the details of the coupling phenomenon are unknown. For instance, real instability mechanisms are often a mixture of mechanism 1 and 2 and not of only one of them. A proposed approach to gain more insights into this instability mechanism is to pulsate the fuel flow rate in a non-premixed

combustor. Multiple studies have examined the behavior of combustors submitted to a pulsation of the air stream to measure their transfer function [15, 21, 22]. Much less data is available for fuel pulsation in non-premixed devices [23].

The objective of this paper is to analyze the response of a swirled non-premixed combustor to a pulsation of the fuel flow rate. The work is performed using Large Eddy Simulation (section 2). The corresponding experimental setup is a 125 kW burner installed at University of Twente (The Netherlands) and described in Section 3. LES and experimental results are first compared for the non-reacting flow (section 4.1). Reacting unforced results are detailed in section 4.2 before presenting results with fuel flow rate pulsation (section 5).

2 Numerical Approach

The LES solver AVBP (see www.cerfacs.fr/cfd) simulates the full compressible multi-species (variable heat capacities) Navier Stokes equations on hybrid grids. Subgrid stresses are described by the classical Smagorinsky model [24]. A two-step chemical scheme is fitted for lean regimes on the GRI-Mech V3 reference [14].

The flame / turbulence interaction is modeled by the Dynamic Thickened Flame (DTFLES) model [25] and allows to handle both mixing and combustion (crucial in partially premixed flames). What the DTFLES model guarantees is that each flame element moves locally at the flame speed corresponding to the equivalence ratio and turbulence level. The flame structure itself obtained ultimately with the DTFLES model has no physical meaning, but the response to acoustic waves or to equivalence ratio perturbations is captured adequately [26].

The numerical scheme uses third-order spatial accuracy and third-order explicit time accuracy [27]. The boundary condition treatment is based on a multi-species extension [28] of the NSCBC method [29], for which the acoustic impedance is fully controlled [30]. The walls are treated as adiabatic, with a law-of-the-wall formulation. Typical runs are performed on grids between $600,000$ and 2.7 million tetrahedra on several parallel architectures (*SGI origin 3800*, *Compaq alpha server*, *Cray XD1*).

3 Computed Configuration

3.1 Target Geometry

The test rig is a 125 kW lab-scale burner developed by University of Twente and Siemens PG in the context of the European Community project DESIRE (Design and Demonstration of Highly Reliable Low Nox Combustion Systems for Gas Turbines).

Figure 2 presents the whole geometry and summarizes the flow path. Figure 3 shows closer views of the various flow passages. The preheated air comes out of the compressor into the air supply room. Then it flows into the plenum through the acoustic decoupling system pipes (Fig. 3-b). After the swirler (Fig. 3-a), the methane is injected in the air cross flow through four small holes to ensure sufficient mixing. Then, the mixture reaches the combustion chamber where the flame is stabilized and burnt gases leave the chamber through the outlet flange (Fig. 3-c).

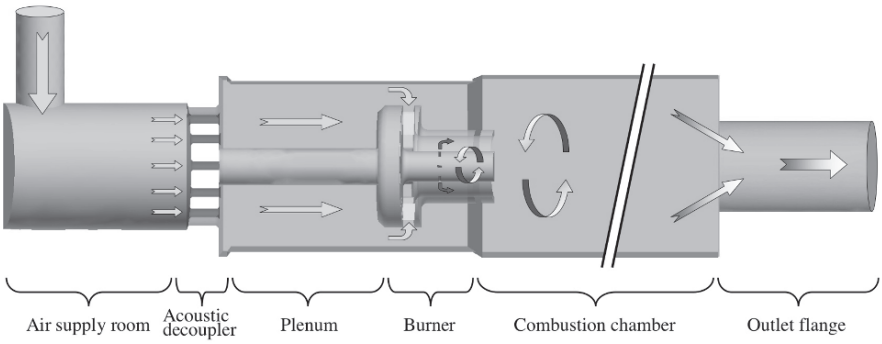

Fig. 2. Full LES computational domain: red, fuel inlet; blue, air inlet; purple, acoustic decoupling system; yellow, swirler vanes; green, outlet flange. (See Plate 42 on page 435)

The LES computational domain (Fig. 2) includes all these upstream parts from the air supply room to the outlet flange. This is necessary to have the right acoustic impedance, to predict accurately the chamber acoustic modes and to minimize the uncertainties on boundary conditions.

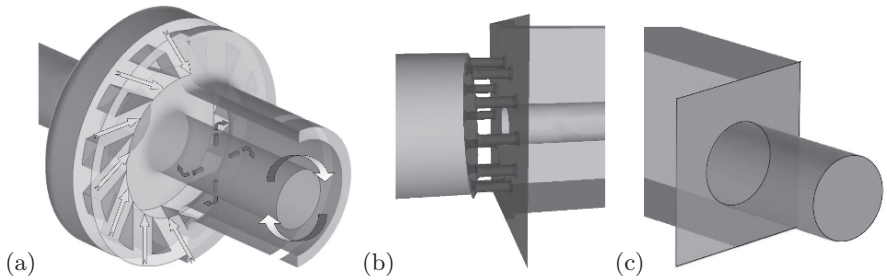

Fig. 3. Details of the computational domain: (a) swirler vanes, (b) acoustic decoupling system and (c) outlet flange. (See Plate 43 on page 435)

3.2 Operating and Boundary Conditions

The operating point simulated is the same for cold, reacting and pulsated flows:

- The air supply room feeds the chamber with 72.4g/s of air, preheated at 573K. This leads to a Reynolds number of 22000 (based on the bulk velocity at the burner mouth and its diameter), and a swirl number [31] of 0.7 (at the same location).
- 3.06 g/s of the natural gas used in industrial gas turbines at ambient temperature (298K) is provided to the fuel line. Note that the so-called "Groningen" natural gas is modeled by a mixture of methane (76.7%) and nitrogen (23.3%) in order to have equivalent thermal properties, so that the global equivalence ratio of the setup is 0.55.
- The mean pressure of the test rig is 1.5 bar.

In the computation, the acoustic behavior upstream the combustion chamber is ensured by the fully reflecting acoustic decoupling system (Fig. 3-b) and downstream the combustion chamber, the impedance at the outlet (Fig. 3-c) is controlled through the NSCBC linear relaxation method [30].

4 Non-Pulsated Cold & Reacting Cases

4.1 Cold Flow Results

The cold flow experiment has been done by University of Twente on a watertunnel based on the Reynolds number similarity. The level of agreement between LES and the experiment is assessed by comparing one dimensional velocity profiles on the central plane at several locations from the burner exit (Plane_A : 5mm, Plane_B : 15mm, Plane_C : 25mm, Plane_D : 45mm and Plane_E : 65mm). Note that the scale employed on all the profiles of a figure is the same. Figure 4 shows the good agreement between experimental data and LES results in both shape and amplitude of the mean velocity components and even on its RMS fluctuations. In particular, the opening angle of the swirled jet, the intensity of central recirculation zone and the re-attachment of the top/bottom recirculation zones are predicted correctly.

4.2 Reacting Flow Results

The steady-state reacting flow and the cold flow dynamics are very similar. The only noticeable difference is the larger opening angle of the swirled jet. Figure 5-(a) exhibits the instantaneous three-dimensional flame structure, materialized by an isosurface of temperature at $1200K$. Even though the flame is compact, it is strongly wrinkled by the turbulence. The corresponding combustion regime is characterized on figure 6 by scatter plots of reaction rate

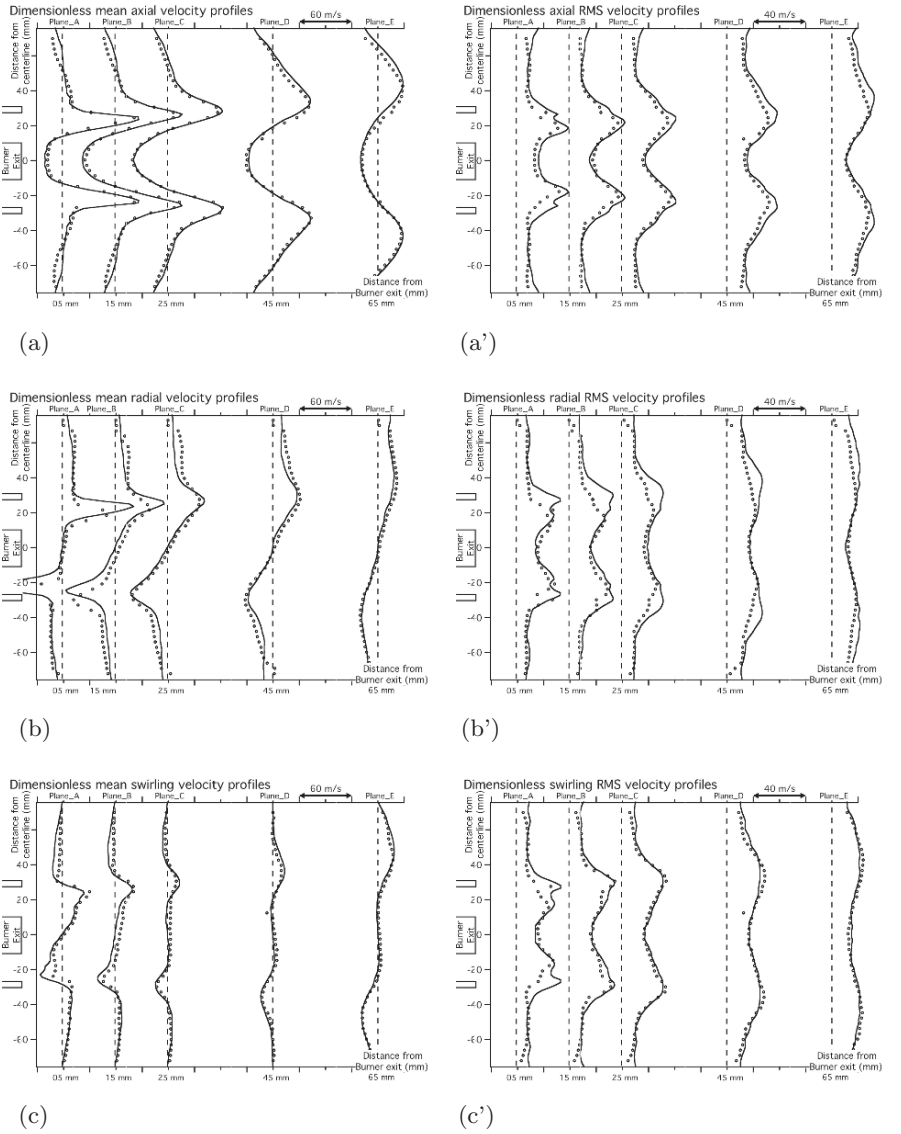

Fig. 4. Comparison of statistical profiles: (a) axial, (b) radial and (c) swirling mean velocity; (a') axial, (b') radial and (c') swirling RMS velocity; Symbols : Experiment; Solid line: LES; dashed line: zero line.

and temperature versus local equivalence ratio (for the whole computational domain). It assesses the quality of the mixing, since very few points burn at equivalence ratio below 0.4 or above 0.7.

The mean location of the flame is shown on figure 5-(b): heat release is exhibited on a longitudinal cut in the central plane. The grey isosurface surrounds the part of the domain where the equivalence ratio ϕ is higher than 0.6. The mean path of the fuel jets in the swirled cross flow is clearly visible. Note that ϕ is computed using passive scalar "z" following [32]. Therefore, it is still valid in burnt gases.

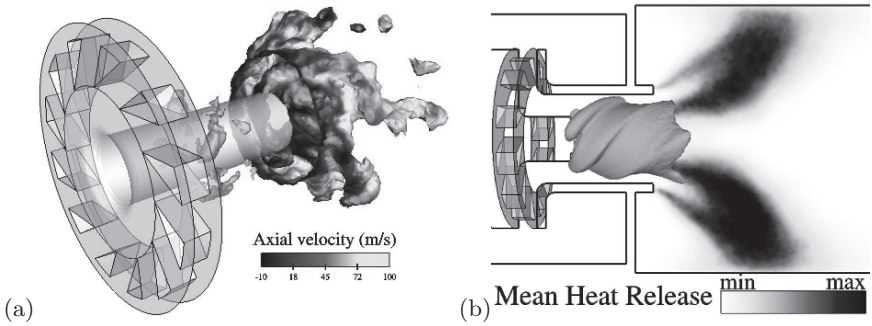

Fig. 5. (a) Instantaneous view of the flame (isosurface of temperature at 1200K) and of the methane jets (isosurface of fuel mass fraction at 0.1); (b) Mean heat release in central plane and isosurface of equivalence ratio $\phi = 0.6$. (See Plate 44 on page 436)

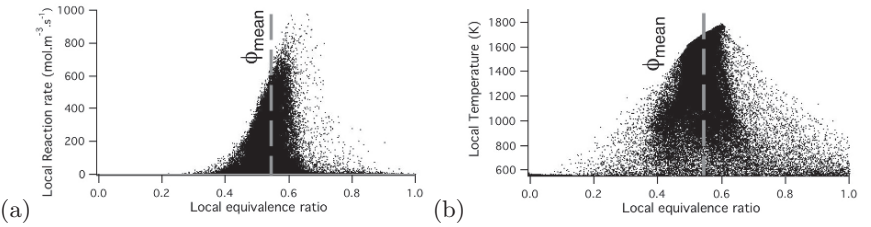

Fig. 6. Combustion regime corresponding to instantaneous solution presented on Fig. 5-a: scatter plots of (a) reaction rate and (b) temperature versus equivalence ratio.

5 Pulsated Reacting Cases

5.1 Forcing Method and Phenomenology

Forcing the reacting flow is achieved by pulsating the mass flow rate of methane in the four fuel pipes (Fig. 3-a). Forcing is performed at 300Hz for

several amplitudes: 5, 10, 15, 30, 50, and 80 percent of the unpulsated mean mass flow rate. For all these amplitudes, the fuel pipes remain subsonic. The mean temporal air flow rate provided by the "air supply room" remains constant, and oscillates instantaneously due to the flow modulations inferred by acoustic waves propagation. Section 5.4 will show that these modulations are not negligible.

Since the momentum of the fuel jets is very small compared to the momentum of the air flow, only the second mechanism described in section 1 is involved. Pulsating the fuel lines should not create ring vortices that could wrinkle the flame and capture pockets of fresh gases. The modulation of fuel flow rate should create alternatively pockets of rich and poor mixture, which after a given convective time will excite the flame. Note that results shown in sections 5.2, 5.3 and 5.4 are related to a pulsation amplitude of 15 percent.

5.2 Acoustic Modes Analysis

A first order acoustic analysis is a simple and powerful tool to understand the mechanisms leading to combustion instabilities. The acoustic eigenmodes of the setup can easily be computed using a 3D Helmholtz code. The field required for this analysis is the local speed of sound and is provided by a temporally averaged solution of the LES.

Table 1 shows the lowest frequencies found numerically, and the corresponding ones measured in the experiment. The agreement between the predicted eigenmodes frequencies and the measured results is reasonable : the Helmholtz code provides higher frequencies for most modes because the mean temperature field was obtained from a LES using adiabatic walls, yielding higher temperature and higher sound speeds.

Table 1. Frequencies computed by the Helmholtz code and measured in the experiment. Physical description of these modes: 1/4 means quarterwave mode. "S" for full Setup, "C" for Chamber and "P" for Plenum.

Frequencies computed (Hz)	72	272	298	487	705	926	1046
Frequencies measured (Hz)	62	192	239	445	630	846	983
Mode description	1/4	5/4	7/4	5/4	7/4	9/4	1/2
Mode related to	S	P	P	C	C	C	P

Coming back to LES, figure 7-(a) now demonstrates that the main peak around 450Hz is clearly captured by LES. This eigenmode of the setup seems to be fed by the flame, especially when the flame is excited by the 300Hz pulsation which is also visible on the LES spectrum (Fig. 7-b). From a physical point of view, it is expected that only the eigenmodes related to the combustion chamber itself may be excited by the flame response. Among these modes, the most sensitive is the closest to the excitation frequency. This is

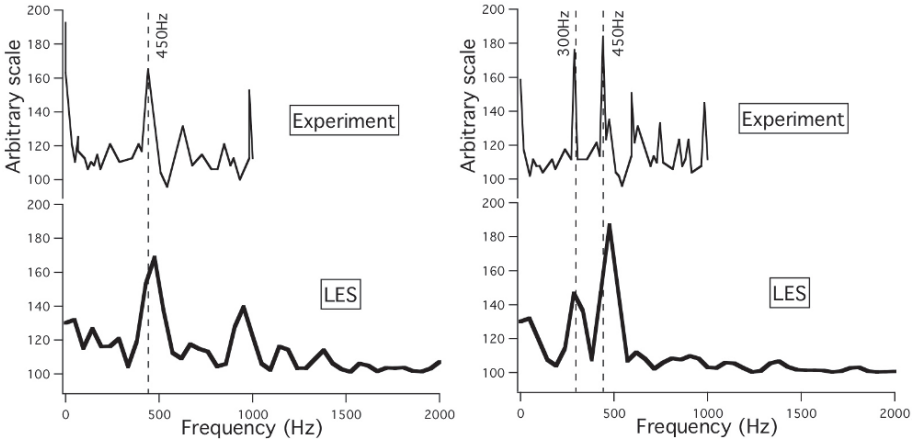

(a) (b)

Fig. 7. Pressure spectra measured in the experiment (thin line) and computed with LES (thick line) for non pulsated (a) and pulsated (b) cases.

why the 450Hz is especially amplified. The other modes near 300Hz (at 72, 272 and 298 Hz) are indeed either eigenmodes of the plenum, or eigenmodes of the full setup. Therefore, they are not sensitive to flame response.

5.3 Phase-Locked Averaged Analysis

Due to the high levels of turbulence which strongly affect the flame (as shown in section 4.2 and figure 5), diagnostic tools are necessary to filter the results. The most obvious one to study harmonic phenomena is the phase-locked averaging procedure.

Figure 8 evidences the shape and intensity of the flame at eight phases of the cycle. It also shows the evolution of rich pockets along this cycle, materialized by an isosurface of equivalence ratio at $\phi = 0.6$ (slightly richer than the mean $\overline{\phi} = 0.55$). After a certain time lag, these pockets reach the reacting zone. The flame does not move significantly when it is reached by these pockets but the local heat release oscillates and triggers the pressure fluctuations feeding the 450Hz acoustic mode (as described in section 5.2).

5.4 Amplification Effect

A controversial question to understand the excitation mechanism is the following: is the air flow rate remaining constant during fuel flow rate pulsation? This can be checked in the LES by evaluating the fuel and air mass flow rates at the mouth of the burner. Using a simple derivation, the variation of the equivalence ratio can be easily split in two parts (Eq. 1): The contribution of instantaneous fuel flow rate to equivalence ratio fluctuations ϕ'_F and the

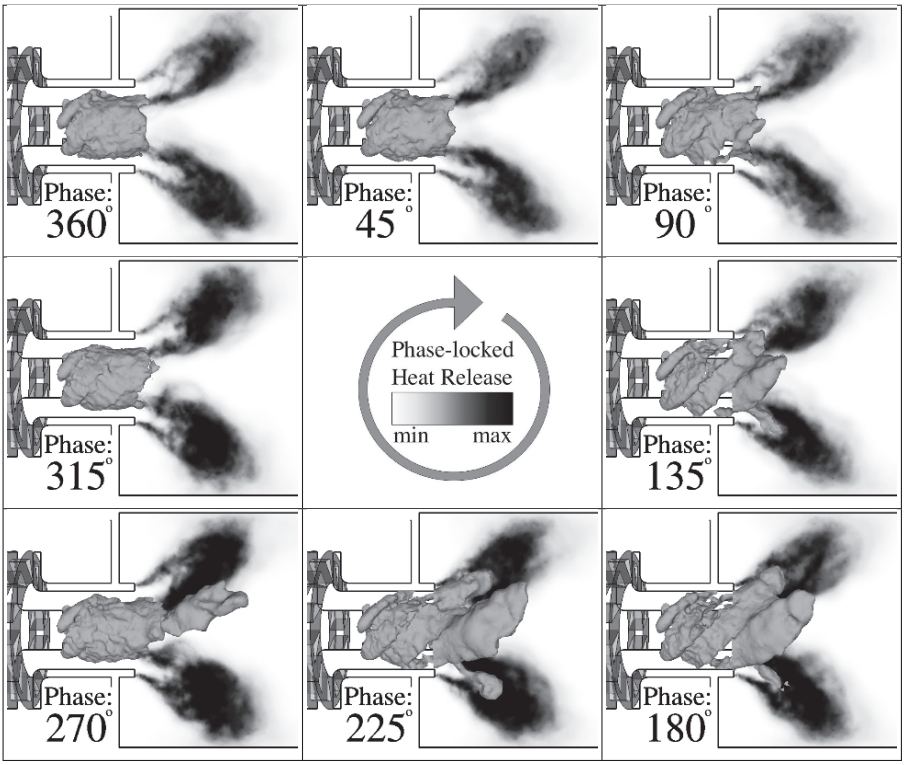

Fig. 8. Phase locked heat release in the central plane and isosurface of equivalence ratio $\phi = 0.6$. (See Plate 45 on page 436)

contribution of instantaneous air flow rate to equivalence ratio fluctuations ϕ'_A.

$$\phi' = \underbrace{\overline{\phi}\frac{\dot{m}_F{}'}{\overline{\dot{m}_F}}}_{\text{Fuel contribution } \phi'_F} \underbrace{- \overline{\phi}\frac{\dot{m}_A{}'}{\overline{\dot{m}_A}}}_{\text{Air contribution } \phi'_A} \tag{1}$$

Figure 9 presents the two contributions ϕ'_F and ϕ'_A for two pulsation amplitudes: 15% and 30%. After a time delay of two cycles, the acoustic waves produced by the flame and partially reflected at the end of the chamber clearly perturb the air flow rate. In other words, the X % pulsation of the fuel line is seen by the flame as a $1.2 \cdot X$ % equivalence ratio excitation. In the present situation and for a forcing frequency of 300Hz, the air flow is also affected by the fuel flow modulation and amplifies its impact on the fluctuations of equivalence ratio at the burner inlet. This conclusion is not general but shows that this effect should be taken into account for modeling.

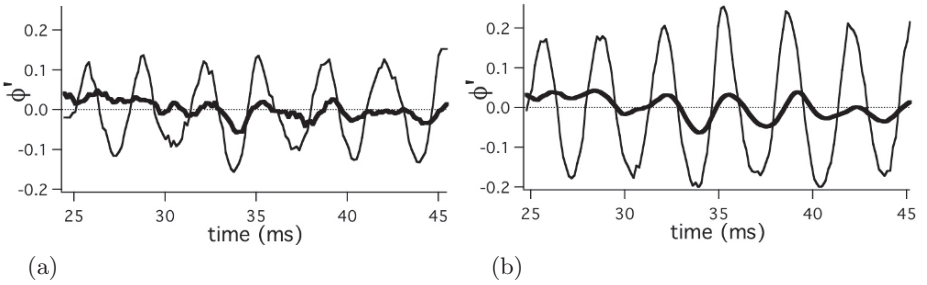

Fig. 9. Contribution of the fuel (thin line) and the air (thick line) fluctuations to equivalence ratio oscillations at the mouth of the burner. The amplitudes of pulsations are: (a) 15%; (b) 30%.

Figure 10 presents scatter plots of local reaction rate versus equivalence ratio at the extrema of the cycle (respectively maximum and minimum global reaction rate). Compared to Fig. 6-(a) (unforced case), the width of the scatter plot is approximately the same which indicates that the effect of forcing on mixing efficiency is not obvious. The distribution of points is just moved alternatively up-right and down-left in the reaction rate - equivalence ratio space.

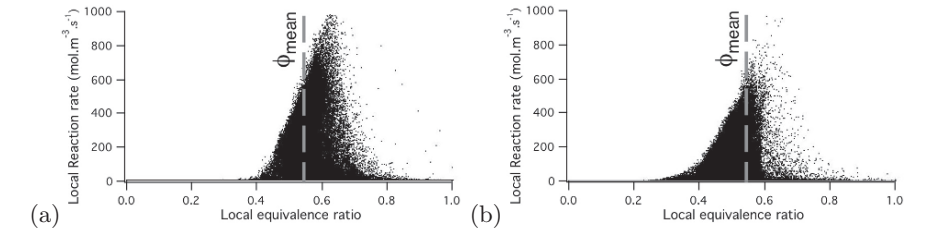

Fig. 10. Combustion regime during the 15% forcing cycle corresponding to (a) maximum reaction rate and (b) minimum reaction rate versus equivalence ratio.

5.5 Saturation Effect

The last point of this paper is the linearity of the flame response to the equivalence ratio pulsation. Recent experimental studies [33, 34] show that beyond a certain pulsation amplitude, a saturation effect is observed. Figure 11 presents the reaction rate fluctuation level for several pulsation amplitudes (Fig. 11-a), up to 80%, and its evolution along the cycle (Fig. 11-b). No saturation effect is noticed here: the flame really behaves linearly within the range considered.

This major difference may be due to the way the equivalence ratio is pulsated: as explained in section 5.1, the pulsation method should not create

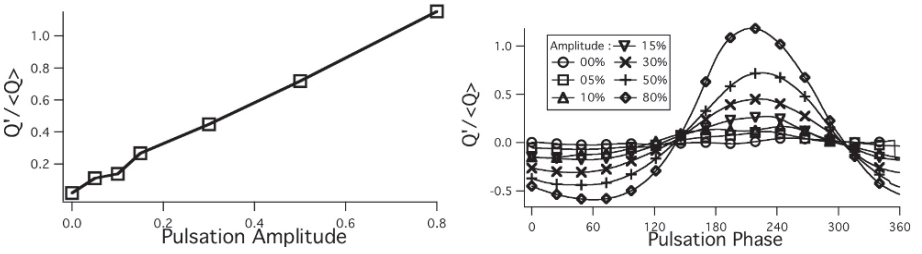

(a) (b)

Fig. 11. Dependence of normalized global heat release fluctuation upon the forcing amplitude (a) and its evolution along the cycle (b).

any ring vortices, so that only the second mechanism described in section 1 is concerned. In Balachandran *et al.*, the fuel flow rate is constant (fuel line choked) and they pulsate the air flow. Therefore, both mechanisms 1 and 2 are involved.

6 Conclusion

Computations of a partially premixed lab-scale burner are carried out using LES for both non-pulsated and pulsated cases. LES results are validated from velocity measurements performed at the University of Twente. The overall agreement with experiment is very good for both mean and RMS values. The mechanism leading to heat release oscillations is characterized using phase-locked analysis and a simple 3D Helmholtz solver. An amplification effect of the equivalence ratio excitations due to reflected acoustic waves perturbing the air flow rate is observed. Note that no saturation effect is noticeable for the range of observation considered, such as presented in Balachandran *et al.* [33, 34]. More generally, this study demonstrated that LES is able to capture the specific role of equivalence ratio fluctuations in phenomena leading to combustion instabilities.

Acknowledgments

Most numerical simulations have been conducted on the computers of *CINES*, French national computing center, consuming about 40,000 hours on a *SGI origin 3800*.

This work was carried out in the framework of the EC project DESIRE with Siemens PG.

References

[1] S. Candel, C. Huynh, and T. Poinsot. Some modeling methods of combustion instabilities. In *Unsteady combustion*, pages 83–112. Nato ASI Series, Kluwer Academic Publishers, Dordrecht, 1996.

[2] F.E.C Culick. Some recent results for nonlinear acoustic in combustion chambers. *AIAA Journal*, 32(1):146–169, 1994.

[3] A.P. Dowling. The calculation of thermoacoustic oscillations. *J. Sound Vib.*, 180(4):557–581, 1995.

[4] A.P. Dowling. A kinematic model of ducted flame. *J. Comput. Phys.*, 394:51–72, 1999.

[5] W. Krebs, P. Flohr, B. Prade, and S. Hoffmann. Thermoacoustic stability chart for high intense gas turbine combustion systems. *Combust. Sci. Tech.*, 174:99–128, 2002.

[6] T. Lieuwen and B.T. Zinn. The role of equivalence ratio oscillations in driving combustion instabilities in low NOx gas turbines. *Proc. of the Combustion Institute*, 27:1809–1816, 1998.

[7] T. Poinsot and D. Veynante. *Theoretical and numerical combustion, second edition*. R.T. Edwards, 2005.

[8] W. Polifke, A. Fischer, and T. Sattelmayer. Instability of a premix burner with nonmonotonic pressure drop characteristic. *J. Engng for Gas Turb. and Power*, 125:20–27, 2003.

[9] T. Schuller, D. Durox, and S. Candel. Self-induced combustion oscillations of laminar premixed flames stabilized on annular burners. *Combust. Flame*, 135:525–537, 2003.

[10] T. Schuller, D. Durox, and S. Candel. A unified model for the prediction of laminar flame transfer functions: comparisons between conical and V-flames dynamics. *Combust. Flame*, 134:21–34, 2003.

[11] H. Pitsch and L. Duchamp de la Geneste. Large eddy simulation of premixed turbulent combustion using a level-set approach. *Proceedings of the Combustion Institute*, 29:in press, 2002.

[12] S. Roux, G. Lartigue, T. Poinsot, U. Meier, and C. Bérat. Studies of mean and unsteady flow in a swirled combustor using experiments, acoustic analysis and large eddy simulations. *Combust. Flame*, 154:40–54, 2005.

[13] V. Sankaran and S. Menon. LES of spray combustion in swirling flows. *J. Turb.*, 3:011, 2002.

[14] L. Selle, G. Lartigue, T. Poinsot, R. Koch, K.-U. Schildmacher, W. Krebs, B. Prade, P. Kaufmann, and D. Veynante. Compressible large-eddy simulation of turbulent combustion in complex geometry on unstructured meshes. *Combust. Flame*, 137(4):489–505, 2004.

[15] A. Giauque, L. Selle, T. Poinsot, H. Buchner, P. Kaufmann, and W. Krebs. System identification of a large-scale swirled partially premixed combustor using LES and measurements. *J. Turb.*, 6(21):1–20, 2005.

[16] T. Poinsot, A. Trouvé, D. Veynante, S. Candel, and E. Esposito. Vortex driven acoustically coupled combustion instabilities. *J. Comput. Phys.*, 177:265–292, 1987.

[17] J. H. Cho and T. Lieuwen. Laminar premixed flame response to equivalence ratio oscillations. *Combust. Flame*, 140:116–129, 2005.

[18] C. Hantschk, J. Hermann, and D. Vortmeyer. Active control with direct drive servo valves in liquid-filled combustion systems. *Proc. Combust. Institute*, 26:2835–2841, 1996.

[19] K. McManus, T. Poinsot, and S. Candel. A review of active control of combustion instabilities. *Prog. Energy Comb. Sci.*, 19:1–29, 1993.

[20] T. Poinsot, D. Veynante, B. Yip, A. Trouvé, J-M. Samaniego, and S. Candel. Active control methods and applications to combustion instabilities. *J. Phys. III*, July:1331–1357, 1992.

[21] W.S. Cheung, G.J.M. Sims, R.W. Copplestone, J.R. Tilston, C.W. Wilson, S.R. Stow, and A.P. Dowling. Measurement and analysis of flame transfer function in a sector combustor under high pressure conditions. In *ASME Paper*, Atlanta, Georgia, USA, 2003.

[22] A. Kaufmann, F. Nicoud, and T. Poinsot. Flow forcing techniques for numerical simulation of combustion instabilities. *Combust. Flame*, 131:371–385, 2002.

[23] D. Bernier, S. Ducruix, F. Lacas, S. Candel, N. Robart, and T. Poinsot. Transfer function measurements in a model combustor: application to adaptative instability control. *Combust. Sci. Tech.*, 175:993–1013, 2003.

[24] J. Smagorinsky. General circulation experiments with the primitive equations: 1. The basic experiment. *Mon. Weather Review*, 91:99–164, 1963.

[25] J.-Ph. Légier, T. Poinsot, and D. Veynante. Dynamically thickened flame large eddy simulation model for premixed and non-premixed turbulent combustion. In *Summer Program 2000*, pages 157–168, Center for Turbulence Research, Stanford, USA, 2000.

[26] P. Schmitt, T.J. Poinsot, B. Schuermans, and K. Geigle. Large-eddy simulation and experimental study of heat transfer, nitric oxide emissions and combustion instability in a swirled turbulent high pressure burner. *J. Comput. Phys.*, in print, 2006.

[27] O. Colin and M. Rudgyard. Development of high-order Taylor-Galerkin schemes for unsteady calculations. *J. Comput. Phys.*, 162(2):338–371, 2000.

[28] V. Moureau, G. Lartigue, Y. Sommerer, C. Angelberger, O. Colin, and T. Poinsot. Numerical methods for unsteady compressible multi component reacting flows on fixed and moving grids. *J. Comput. Phys.*, 202:710–736, 2005.

[29] T. Poinsot and S. Lele. Boundary conditions for direct simulations of compressible viscous flows. *J. Comput. Phys.*, 101(1):104–129, 1992.

[30] L. Selle, F. Nicoud, and T. Poinsot. The actual impedance of non-reflecting boundary conditions: implications for the computation of resonators. *AIAA Journal*, 42(5):958–964, 2004.

[31] A.K. Gupta, D.G. Lilley, and N. Syred. *Swirl flows*. Abacus Press, 1984.
[32] J.-Ph. Légier. *Simulations numériques des instabilités de combustion dans les foyers aéronautiques*. PhD Thesis, INP Toulouse, 2001.
[33] R. Balachandran, B. O. Ayoola, A. P. Kaminski, A. Dowling, and E. Mastorakos. Experimental investigation of the non-linear response of turbulent premixed flames to imposed inlet velocity oscillations. *Combust. Flame*, 143:37–55, 2005.
[34] R. Balachandran, A. Dowling, and E. Mastorakos. Response of turbulent premixed flames to inlet velocity and equivalence ratio perturbations. In *European Combustion Meeting*, 2005.